

# Saturation regimes at LHC energies

J.-R. Cudell, O. V. Selyugin<sup>1</sup>

*Institut de Physique, Université de Liège, Belgium* %todayempty

## Abstract

The effects of saturation and unitarization for hadron-hadron scattering at LHC energies are explored in several models. It is shown that different choices of saturation parameters lead to sizable differences in the energy dependence of total cross sections, and to dramatic changes in elastic differential cross sections.

## 1 Introduction

Saturation is now a very popular term, and it has a very wide meaning. It includes “shadowing” and “anti-shadowing” processes, gluon saturation, unitarization, etc. In this paper, by “saturation” we mean that the “black disk” limit (BDL) has been reached, and that effects connected to the unitarity of the scattering amplitude must be taken into account.

Standard ingredients for the discussion of this regime can be found, e.g. in the loop-loop correlation model [1], which is based on a functional integral approach to high-energy collisions [2]. Here, the  $T$ -matrix element for elastic scattering is given by the correlation function of two light-like Wigner-Wilson loops:

$$\begin{aligned} T_{pp}(s, t) &= 2is \int d^2 b_\perp e^{i\vec{q}_\perp \cdot \vec{b}} J_{pp}(s, |\vec{b}|) \\ \text{with } J_{pp}(s, |\vec{b}|) &= \int dz_1 d^2 r_1 \int dz_2 d^2 r_2 |\psi_p(z_1, \vec{r}_1)|^2 |\psi_p(z_2, \vec{r}_2)|^2 \\ &\quad \times [1 - S_{DD}(s, \vec{b}, z_1, \vec{r}_1, z_2, \vec{r}_2)] \end{aligned} \tag{1}$$

---

<sup>1</sup>BLTPh, JINR, Dubna, Russia.

The saturation of the profile function  $J_{pp}$  appears then as a manifestation of the unitarity of the  $S$ -matrix.

Whether the BDL will affect LHC physics, and how it is reached in QCD is still a matter of debate. For instance, if we consider its effect on the total cross section  $\sigma_{tot}$  (which can be obtained directly from  $T_{pp}$ ), the standard point of view is that the saturation of  $J_{pp}(s, |\vec{b}|)$  tames its growth: there is a transition from a power-like to an  $\ln^2(s)$ -increase of  $\sigma_{pp}^{tot}(s)$ , which then respects the Froissart bound

But where this effect will take place is not clear: the analysis of [1] predicts that the saturation regime at small  $b$  is reached only at very small  $x \approx 10^{-10}$  and very high energies  $\sqrt{s} \geq 10^6$  GeV. Thus – according to this model – the onset of the BDL in  $pp$  collisions is about two orders of magnitude beyond LHC energy. However, other authors (see e.g. [3]) predict the same effect, within the dipole picture of soft processes, but at much lower energies.

The connection with unitarisation becomes clear if we notice that the eikonal representation for the scattering amplitude in  $\vec{b}$ -space, in the form  $1 - \exp(-\chi(s, b))$ , reaches the BDL only asymptotically. However, this representation is not the only possibility, and it may be more useful to consider the effects of saturation by considering parametrisations in  $s$  and  $t$ , transforming them to impact parameter space, and imposing the BDL as an upper bound on the amplitude in  $s$  and  $b$ .

## 2 Donnachie -Landshoff (DL) model

Hence, we shall first consider this approach in the DL model, which must certainly be unitarized at high energies. Here, the  $pp$ -elastic scattering amplitude is proportional to the hadronic form factors, and can be approximated at small  $t$  by:

$$T(s, t) = h_0 s^\epsilon e^{D t} e^{\alpha' t \ln s}. \quad (2)$$

Going to impact parameter space, we obtain the 1-pomeron amplitude  $\Gamma_1(b, s)$ :

$$\Gamma_1(b, s) = h_0 \frac{(s/s_0)^\epsilon}{2 [4 + \alpha' \ln s/s_0]} \exp\left(-\frac{b^2}{4(4 + \alpha' \ln s/s_0)}\right), \quad (3)$$

with  $h_0 = 4.7 \text{ GeV}^{-2}$ ;  $\epsilon = 0.0808$ ;  $\alpha' = 0.25 \text{ GeV}^{-2}$ ;  $D = 4 \text{ GeV}^{-2}$  and  $s_0 = 1 \text{ GeV}^2$  ( $s_0$  will be dropped below). Double-pomeron exchange then gives:

$$\Gamma_2(b, s) = \Gamma_1(b, s) - \lambda \Gamma_1^2(b, s)/2$$

At some energy and at small  $b$ ,  $\Gamma_1(b, s)$  and  $\Gamma_2(b, s)$  reach the BDL (see Fig. 1). For one-pomeron exchange, this happens at  $\sqrt{s} = 1.5 \text{ TeV}$  whereas the 2-pomeron exchange term moves the limit up to  $\sqrt{s} = 4.5 \text{ TeV}$  (for  $\lambda = 0.2$ ).

The details of the saturation process are very important at super-high energies. In Fig. 2, we show different ways to implement saturation at  $\sqrt{s} = 14 \text{ TeV}$ : the solid line shows  $\Gamma_1$  without saturation; the dashed line corresponds to the “hard cut” case, where we simply freeze  $\Gamma_1$  at 1, which corresponds to a specific point where the curve has a knee; the dash-dotted curve and the circles represent the above cases for  $\Gamma_2$ . Simply freezing  $\Gamma$  breaks analyticity, hence we must consider scenarios where the BDL is smooth. First of all, we can continue the  $\Gamma = 1$  plateau by a Gaussian which connects quickly to the original curve (“soft cut”). Secondly, we shall consider a (“scaling”) case: once  $\Gamma$  reaches 1, we assume that the factor multiplying the exponential in Eq. (3) is renormalised to 1, but the curve gets shifted towards higher values of  $b$ , such that the growth of the radius (defined as the point at which  $\Gamma = 1/2$ ) remains the same as in the unsaturated curve. This gives us a smooth growth of the saturated core, as shown by the dotted curve in Fig. 2. Although it slightly changes the form of  $\Gamma$  near the knee, it gives the same asymptotic behaviour at large  $b$ .

Fig. 3 shows the consequences of the above saturation schemes on  $\sigma_{tot}$ . The solid line corresponds to the case without saturation, the dash-dotted line to the “hard cut”, the dashed line to the “soft cut” and the dash-dotted-dotted line to the “scaling” case. Fig. 3 also gives the results of full eikonalization ( $\Gamma(b, s) = 1 - \exp[-1.233 \Gamma_1(b, s)]$ ) as a long dashed line and of the Dynamic Peripheral Model (DPM) [5] as a dotted line. We see that  $\sigma_{tot}$  does not depend much on the details of saturation at LHC energies, whereas at very large energies a sizable fraction of the cross section will come from these, and hence from the hadron structure at large distances.

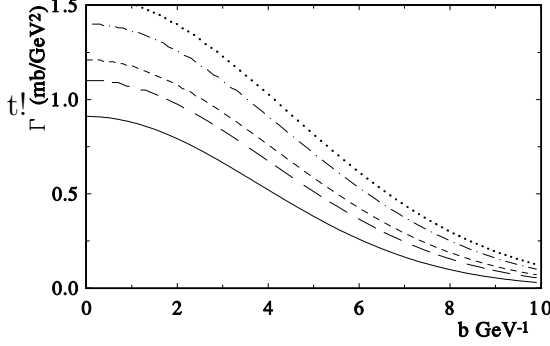


Fig. 1: The  $s$  and  $b$  dependence of  $\Gamma_1$

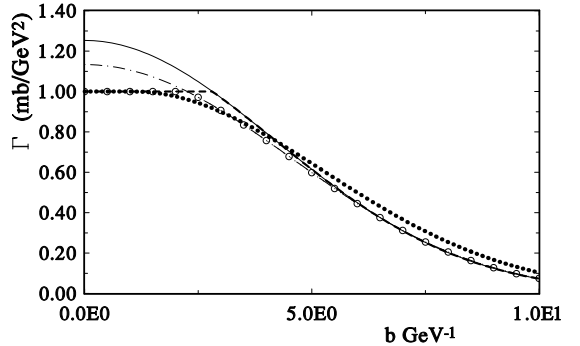


Fig. 2:  $\Gamma_1$  and  $\Gamma_2$  at 14 TeV  
(see explanation in text)

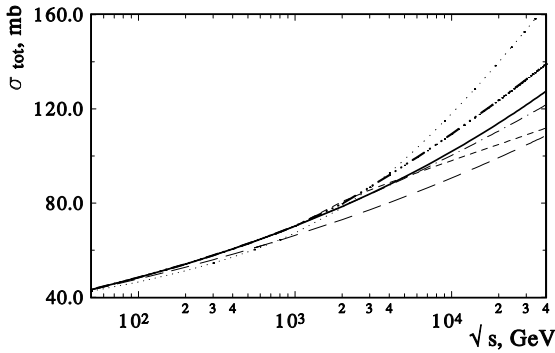


Fig. 3: The different predictions of  $\sigma_{tot}$  (see explanation in text)

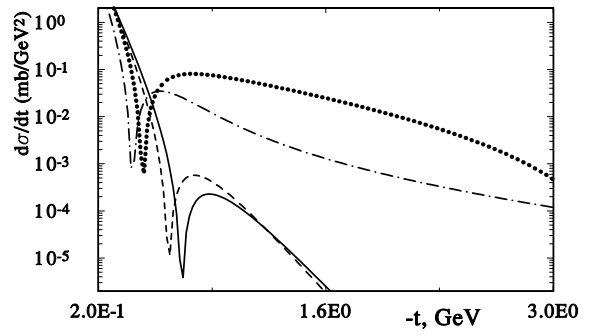


Fig. 4:  $d\sigma/dt_{pp}$  in the  $pp$  case, at 4 and 14 TeV.

At the LHC, the effects of saturation can however be observed in elastic scattering. Fig. 4 shows that the saturation effects can lead to a large increase in the differential cross section at large  $|t|$ . The solid and long-dashed lines represent  $d\sigma/dt$  at 4 and 14 TeV, without saturation. The dash-dotted line and the points show  $d\sigma/dt$  at 14 TeV in the “hard cut” and “scaling” cases. Both scenarios, while giving different predictions for the growth of  $\sigma_{tot}$ , lead to a similar large growth of the differential cross section. Note that we do not aim here at quantitative predictions, but only want to gauge possibilities.

### 3 The Dynamic Peripheral Model

We can compare the above results with those of the eikonal dynamical model of  $hh$ -scattering developed in [5]. The model is based on the general principles of quantum field theory

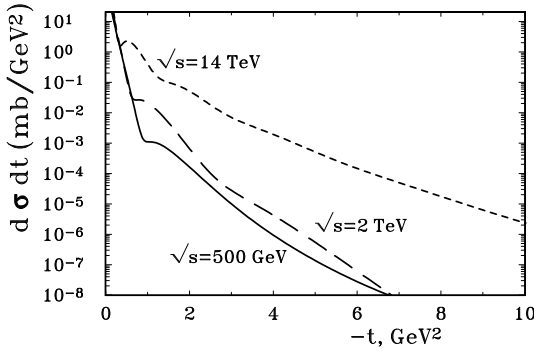


Fig. 5:  $d\sigma/dt$  from the DPM in the  $pp$  case.

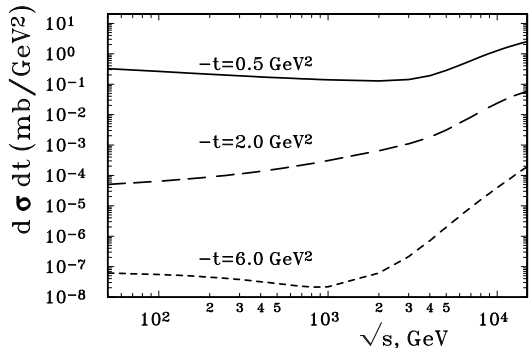


Fig. 6:  $d\sigma/dt$  from the DPM in the  $pp$  case at fixed  $t$ .

(analyticity, unitarity, causality ) and takes into account basic information on the structure of a hadron as a compound system, with a central region in which the valence quarks are concentrated and with a long-distance region occupied by the color-singlet quark-gluon field. The model provides a self-consistent picture of  $d\sigma/dt$  and of spin phenomena for different hadron processes.

The predictions of the DPM for elastic  $pp$ -scattering at  $\sqrt{s} = 53$  GeV and 14 TeV are shown in Fig. 5. At high energies, one can see that  $d\sigma/dt$  changes its behavior and grows with increasing energy. This can be seen in more details in Fig. 6. This effect is due to the peripheral term which comes from the interaction of the pomeron with the two-pion cut and leads to a growth of  $\sigma_{tot}$  as  $\sim (\ln s)^2$  and to a rapid growth of  $d\sigma/dt$  at large  $|t|$ . It is evident that the growth of the size of proton increases the role of peripheral effects at super-high energies, where the BDL is reached. After that,  $d\sigma/dt$  changes behavior and begins to grow at fixed  $t$ .

## 4 Conclusion

We have shown that the saturation effects, in very different approaches, may be observable at the LHC. They lead on the one hand to a change in the monotonic behavior of  $\sigma_{tot}$  and, on the other, to an increase of  $d\sigma/dt$  at large  $|t|$ . Hence the LHC experiments may tell us if we reached the saturation regime, and provide information on the hadron dynamics at large distances.

The authors would like to thank P. Landshoff for helpful discussions. O.V.S. is a Visiting Fellow of the Fonds National pour la Recherche Scientifique, Belgium.

## References

- [1] A. I. Shoshi and F. D. Steffen, arXiv:hep-ph/0212070.
- [2] O. Nachtmann, Annals Phys. **209** (1991) 436; H. G. Dosch, E. Ferreira and A. Kramer; Phys. Rev. D **50** (1994) 1992 [arXiv:hep-ph/9405237].
- [3] J. Bartels, E. Gotsman, E. Levin, M. Lublinsky and U. Maor, Phys. Lett. B **556** (2003) 114 [arXiv:hep-ph/0212284].
- [4] A. Donnachie and P. V. Landshoff, Nucl. Phys. B **231** (1984) 189.
- [5] S. V. Goloskokov, S. P. Kuleshov and O. V. Selyugin, Z. Phys. C **50** (1991) 455.